2021 43rd Annual International Conference of the
IEEE Engineering in Medicine & Biology Society (EMBC)
Oct 31 - Nov 4, 2021. Virtual Conference

Design Analysis and Circuit Topology Optimization for Programmable Magnetic Neurostimulator

Majid Memarian Sorkhabi*, Frederick Gingell, Karen Wendt, Moaad Benjaber, Kawsar Ali, Daniel J. Rogers, and Timothy Denison

Abstract— **Transcranial magnetic stimulation (TMS) is a form of non-invasive brain stimulation commonly used to modulate neural activity. Despite three decades of examination, the generation of flexible magnetic pulses is still a challenging technical question. It has been revealed that the characteristics of pulses influence the bio-physiology of neuromodulation. In this study, a second-generation programmable TMS (xTMS) equipment with advanced stimulus shaping is introduced that uses cascaded H-bridge inverters and a phase-shifted pulse-width modulation (PWM). A low-pass RC filter model is used to estimate stimulated neural behavior, which helps to design the magnetic pulse generator, according to neural dynamics. The proposed device can generate highly adjustable magnetic pulses, in terms of waveform, polarity and pattern. We present experimental measurements of different stimuli waveforms, such as monophasic, biphasic and polyphasic shapes with peak coil current and the delivered energy of up to 6 kA and 250 J, respectively. The modular and scalable design idea presented here is a potential solution for generating arbitrary and highly customizable magnetic pulses and transferring repetitive paradigms.**

I. Introduction

Transcranial Magnetic Stimulation (TMS) uses electromagnetic induction to modulate neural activity. It is used as both an FDA-approved treatment for depression and major depressive disorder [1] as well as an important diagnostic tool for neurological disorders. The stimulation coil is positioned over the appropriate cortex site and a high voltage pulse is applied to it. The induced magnetic field drives a brief current in the brain which either directly generates action potentials through depolarization or modifies the state of cortical excitability [2].

Altering stimulation parameters such as pulse magnitude and pulse rate gives increased flexibility to investigate the brain in a safe, non-invasive manner. However, conventional TMS systems are limited by the lack of flexibility of their electrical architecture, and therefore can only produce damped cosine pulses [1]. For each pulse, a thyristor triggers an energy-storage capacitor (C) to discharge to the inductive stimulation coil (L), generating a short, fixed cosine magnetic pulse. The values of L and C control the resonance frequency, and thus the pulse duration. Over time, several modifications to this architecture have been suggested. Notably, the controllable TMS (cTMS) devices [3] can achieve a slightly wider variety of near-rectangular pulses by using insulated-gate bipolar transistors (IGBTs) to deliver variable width pulses.

A proof-of-concept solution, able to produce an even broader range of pulse shapes, has been described in our first programmable TMS (pTMS) concept [4]. It uses an H-bridge with switching elements that utilize a pulse width modulation (PWM) technique to approximate any arbitrary voltage pulse within its magnitude. An RC circuit model was used to estimates the intrinsic neural response to a PWM-equivalent pulse [5] [6], which was shown to be close to the neural response to a conventional TMS pulse of the same magnitude. Although it expanded the range of possible pulse shapes, our first pTMS prototype was not able to achieve higher voltage pulses. The peak voltage of a 2.5 kHz conventional biphasic TMS pulse reached around 1000 V, which is equal to 63% of the maximum stimulator output (MSO) for standard TMS devices. Increasing the DC-link voltage could exceed the breakdown voltage of high current IGBTs and cause a collector-to-emitter breakdown.

This provides a motivation to investigate whether, by adding more H-bridges to the inverter, the second-generation of the programmable TMS (xTMS) device could mimic these higher voltage TMS pulses, as well as providing higher accuracy pulses. The 'x' aims to represent the increased range of pulses this second-generation device can achieve. The extent to which increasing the number of H-bridges (called cascaded H-bridge inverter or CHB) will improve the xTMS system performance is investigated in this paper. A simulation is created to compare the 3-level system (one CHB) against a 5-level (two CHB) and a 7-level (three CHB) system. The result is then used to inform the design of a second prototype.

II. Method

A. Principle of operation

The conceptual block diagram of the proposed xTMS device is shown in Figure 1. The key architectural feature of the proposed system is the use of PWM to imitate an arbitrary

* This work was supported by a programme grant from the MRC Brain Network Dynamics Unit at Oxford, as well as supplemental funding to Denison by the Royal Academy of Engineering and Wendt by an MRC iCASE fellowship.

* M. Memarian Sorkhabi, K. Wendt, Moaad Benjaber and T. Denison are members of the MRC Brain Network Dynamics Unit, University of Oxford, Oxford, OX1 3TH, UK (e-mail: majid.memariansorkhabi@ndcn.ox.ac.uk, karen.wendt@some.ox.ac.uk, moaad.benjaber@bndu.ox.ac.uk). Frederick Gingell, Kawsar Ali, D. Rogers and T. Denison are affiliated with the Department of Engineering Science, University of Oxford, Oxford, OX1 3PJ, UK (e-mail: frederick.gingell@magd.ox.ac.uk,kawsar.ali@eng.ox.ac.uk,dan.rogers@eng.ox.ac.uk, timothy.denison@eng.ox.ac.uk). Introduced technology and method are subject of patent application by University of Oxford. For the purpose of Open Access, the authors have applied a CC BY public copyright license to any Author Accepted Manuscript version arising from this submission.

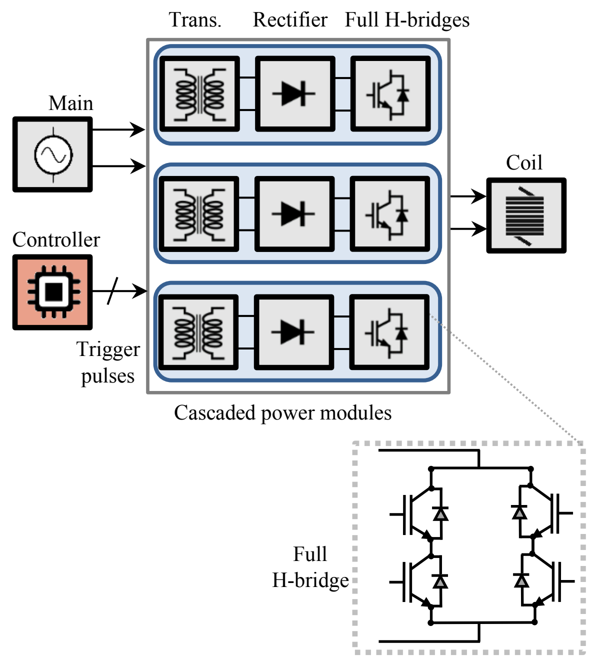

Figure 1 The overall diagram of the proposed xTMS system

waveform stimulus [5]. The desired reference waveform is the input to a controller, which uses Unipolar PWM (U-PWM) to trigger IGBTs in a stacked H-bridge layout [6]. The voltage produced is a multi-step approximation to the reference waveform. The core components are similar to traditional AC-AC inverters, which first transform input AC voltage up to a higher voltage level by a step-up transformer(s), then rectify it, before connecting to the high capacitance DC link capacitor(s), which maintain a certain input voltage for the inverter [7]. The generated trigger pulses, which are based on the U-PWM approach, continuously turn on/off the CHBs' switches and mimic the desired pulse. The structure of the H-bridge and the inductive load can return the delivered energy from the coil to the DC capacitors and improve the efficiency of the proposed TMS system.

Modularity at the inverter level is one of the key concepts enabling scalability, flexibility and leads to standardization of modules of the TMS solution. Increasing the number of CHB modules and DC links improves the number of stimulus voltage levels; a cascade of 'n' H-bridges can produce (2n + 1) voltage levels at the PWM-based stimulus. Although increasing the circuit elements makes the system bulkier and more complex, the shape of the generated stimulus will ideally be closer to the desired reference waveform.

B. *Simplified circuit topology*

The three circuits for the 3/5/7-level xTMS circuits were modelled in MATLAB Simulink software (Powergui blockset). The D70 remote coil (Magstim Company Ltd, Wales) with a 15.5 µH inductance and a 20 mΩ parasitic resistance is set for all structures. The H-bridge module is shown in Figure 1 inset. The IGBTs are modelled as non-ideal switches with equivalent parasitic internal resistance (R_{on}= 1.5 mΩ) and local capacitors between collector-emitter (1 µF). The DC-link is modelled as a current source which, given the high capacitance of the DC link capacitor, is equivalent to an AC-DC converter. The DC-link capacitance was chosen for each circuit to ensure that voltage V_{DC} would remain above 95% of its initial charged value throughout a standard 400 µs biphasic stimulus.

In order to compare the 3-level, 5-level and 7-level configurations, each controller followed the same reference pulse, a 2.5 kHz 1000 V_{pp} cosine wave. Note that due to circuit losses, the magnitude of a conventional biphasic TMS wave reaches around only 80% of its initial voltage by the end of the pulse. The switching frequency for each H-bridge was chosen to be 10 kHz. Thus, the effective switching frequency is 20 kHz for the 5-level simulation, and 30 kHz for the 7-level simulation. An increase in switching frequency indicates that unwanted harmonics are being pushed to higher frequencies as the number of H-bridges increases.

C. *Neural response model*

An important characteristic of the neural membrane is the filtering of high-frequency voltages. The physiological response to the xTMS PWM stimulus was therefore modelled as a low-pass filter to estimate the membrane voltage change after a magnetic stimulation. Barker et al. estimated the time constant of the neural membrane as τ = RC = 150 µs, where R represents the membrane effective resistance and C, the effective membrane capacitance [8]. This simple model allows us to compare the predicted physiological response of a conventional TMS system to a xTMS (2n+1)-level PWM variant.

D. *Simulation results*

Figure 2 compares the ideal reference and actual xTMS output pulse for both the coil voltage (V_{COIL}), and the modelled membrane voltage change (ΔV) for reference (ideal) and the 3, 5 and 7-level xTMS configurations for a 2.5 kHz biphasic pulse. It is noteworthy that the pTMS technology can mimic different pulse waveforms such as near-rectangular, monophasic, and biphasic pulses, which are generated by other TMS devices. The L^2 norm of the dissimilarity between the reference pulse and the PWM-equivalent pulse is tabulated in Table 1 for quantitative comparison, where the L^2 norm for the coil voltage is:

$$\|D_{coil}\|_2 = \sqrt{\frac{1}{t_1}\int_0^{t_1} |V_{REF}(t) - V_{COIL}(t)|^2 dt} \quad (1)$$

and the L^2 norm for the membrane voltage change is:

$$\|D_{membrane}\|_2 = \sqrt{\frac{1}{t_1}\int_0^{t_1} |\Delta V_{REF}(t) - \Delta V_{PWM}(t)|^2 dt} \quad (2)$$

where $\Delta V_{REF}(t)$ and $\Delta V_{PWM}(t)$ are the membrane voltage changes for the ideal reference pulse and the PWM-equivalent pulse, respectively. A value closer to 0 indicates that the xTMS generates a similar response to that of the defined (smooth) reference.

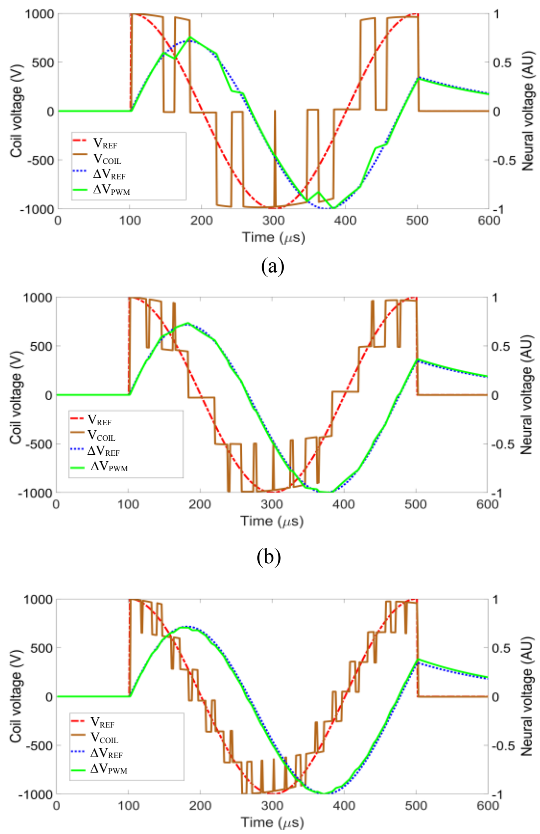

(c)

Figure 2 Simulation of the applied PWM coil voltage together with the ideal (ΔV_{REF}) and approximated behavior of a neuronal membrane voltage (ΔV_{PWM}) during magnetic stimulation for: (a) 3-level PWM stimulus. (b) 5-level PWM stimulus and (c) 7-level PWM stimulus.

TABLE 1 L^2 NORM FOR DIFFERENT PULSE SHAPES

Reference stimulus shape		3-level	5-level	7-level
Biphasic	$\|\|\boldsymbol{D_{coil}}\|\|_2$	0.31	0.15	0.12
	$\|\|\boldsymbol{D_{membrane}}\|\|_2$	0.058	0.021	0.033
Monophasic	$\|\|\boldsymbol{D_{coil}}\|\|_2$	0.28	0.17	0.13
	$\|\|\boldsymbol{D_{membrane}}\|\|_2$	0.046	0.036	0.045
Square	$\|\|\boldsymbol{D_{coil}}\|\|_2$	0.13	0.13	0.13
	$\|\|\boldsymbol{D_{membrane}}\|\|_2$	0.013	0.011	0.015
Half Sine	$\|\|\boldsymbol{D_{coil}}\|\|_2$	0.16	0.083	0.074
	$\|\|\boldsymbol{D_{membrane}}\|\|_2$	0.050	0.057	0.065

E. Cost-Benefit analysis

Table 2 compares the efficiency of each of the systems considered. The power switch loss includes Thyristor conduction loss (conventional TMS) or IGBT switching/conduction losses ((2n+1)-level PWM). The total loss also includes coil copper losses. To reduce the current stress on the IGBTs, three switches are in parallel in each leg of the H-bridge.

The cost of each system's switching components, which is one of the main hardware costs, is used in Table 2 to compare total build cost; this is the thyristor (conventional TMS) or the IGBTs ((2n+1)-level PWM). The simulated circuits demonstrate both costs and benefits of increasing the number of H-bridges beyond the singular H-bridge. Although accuracy of waveform and total achievable voltage magnitude increases with the number of H-bridges, power loss and cost-to-build increases as well. These trade-offs are summarized in Table 2. It should be noted that the cost of DC capacitor chargers is not included in this table. By increasing the number of H-bridges, the number of required chargers will also increase.

The efficiency of the xTMS decreases with the increase in number of H-bridges, since the switching and conduction losses of each module are increased by growing the circuit size. Evidently, the cost-to-build increases with the number of CHBs. The maximum voltage of a conventional TMS is 1650V [9] [10], and so the 5-level xTMS and the 7-level xTMS are both able to reach the conventional TMS pulses. The 7-level system is more accurate at replicating the reference waveform, despite the decrease in supply voltage as a result of extra impedances in the third CHB.

The modeling results and calculations show that changing the number of PWM voltage levels from 3 to 5 can have a significant positive effect on the similarity of the PWM-based TMS pulse and reference pulse, as well as on the membrane voltage changes. Increasing further up to 7-level PWM system, however, does not show any notable improvement of the L^2 norm compared to a 5-level PWM system. On the other hand, the use of the three cascaded power modules to build a 7-level PWM system increases the complexity, cost-to-build and dimensions of the final device. A 7-level system, therefore, is more suited for high power applications. For conventional 1650V TMS applications, choosing a 5-level PWM-based TMS device for prototyping seems optimal.

III. IMPLEMENTED NEUROSTIMULATOR

The details of implementing the proposed xTMS device to generate 5-level PWM magnetic pulses are as follows. The primary circuit components used in the implementation are

TABLE 2: COMPARISON OF THE POWER LOSS AND THE EFFICIENCY OF DIFFERENT TMS SYSTEMS

(Biphasic 400 μs pulse)	Power switch loss per pulse (J)	Total loss per pulse (J)	Efficiency (%)	Achievable max coil voltage (V) (peak)[1]	MSO (Joules)[2]	Cost of high voltage switches (£)[3]
Conventional TMS	3.5	52	93	1650	250	91
3-level PWM	7.9	57	92	1000	100.4	1432
5-level PWM	16	65	91	1920	380	2865
7-level PWM	24	73	90	2880	775	4300

[1]Based on 20% safety margin for the selected-IGBT collector-emitter breakdown voltage.
[2]Achievable Maximum device output (regardless of the nominal IGBT current)
[3]High voltage switches in a conventional TMS include one thyristor (£91 [11]) and in the xTMS include 6 IGBT modules (£238.78 each [12]) per full H-bridge.

shown in Table 3 and the laboratory xTMS setup is represented in Figure 3. An autotransformer is used to adjust the charging voltage of the DC capacitors and the intensity of the magnetic stimulus. Control buttons are utilized to energize the autotransformer (start button), to start charging the DC capacitors (arm button) and to de-energize the autotransformer and discharge the DC capacitors (discharge button). Panel meters measure the DC link voltages and the capacitor charging currents. The emergency stop button is used to cut off the input power and mains supply and to discharge the DC capacitors. The xTMS system has been designed to comply with the BS EN 60601-1:2006+A12:2014 (Medical electrical equipment - Part 1: General requirements for basic safety and essential performance) and BS IEC 60601-1-4-2000 (General Requirements for Safety - Collateral Standard: Programmable Electrical Medical Systems) standards. The coil temperature was monitored by reading the temperature sensors embedded in each side of the coil.

A. AC/DC converter stage:

The two isolated AC/DC converters contain step-up transformers, full-wave diode rectifiers, and pulse (energy storage) capacitors. These capacitors are charged up to V_{DC}= 800 V and the output pulse amplitude (stimulation intensity) is adjusted by the variable autotransformers.

B. DC/AC inverter stage

The proposed xTMS device uses 32 IGBTs in the form of two cascaded H-bridges (3 parallel IGBT modules in each leg, totaling 12 modules for the DC/AC inverter block) whose outputs are connected to the stimulation coil, as shown in Figure 1. Custom-designed gate drivers are used to drive the parallel-connected IGBTs and to reinforce equal current sharing between the parallel-connected switches, more details can be found in [13]. The Micro Lab Box commercial control system is used to generate trigger pulses for the drivers at a precision of 10 ns.

C. Experimental measurements and results

Measurement results of three different stimulus waveforms are exhibited in Figure 4. The coil voltage and coil current were measured via a high-voltage differential probe (TA044, PICO TECHNOLOGY, UK) and a Rogowski current probe (I6000S FLEX-24, FLUKE, USA), respectively. The proposed two-cell architecture was tested with a maximum DC link voltage of V_{DC1} = V_{DC2} = 800 V. For a 2.5 kHz cosine pulse, the maximum energy delivered to the stimulation coil was measured to be 250 joules, which is equal to 100% of MSO, in the form of biphasic wave. The achievable frequency starts at 2 kHz and can be increased up to 5 kHz.

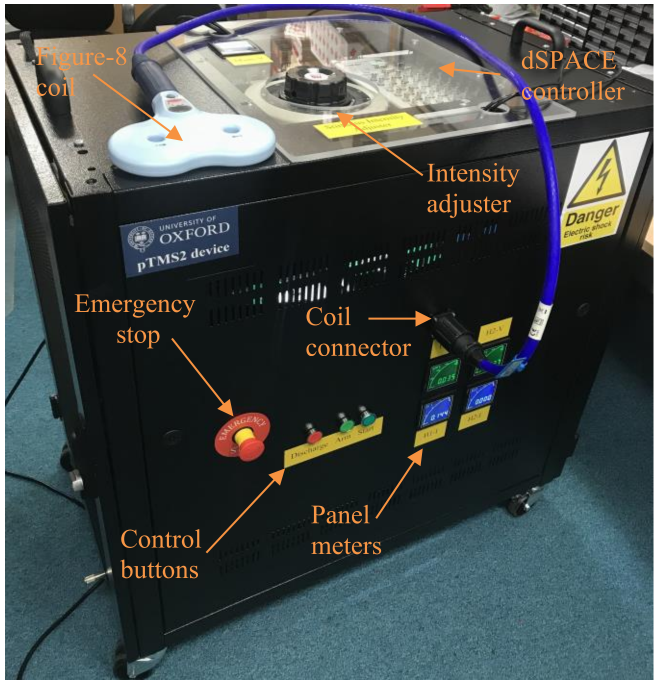

Figure 3 xTMS prototype

IV. DISCUSSION

Power converters have been gaining popularity in neurostimulator devices owing to their potential to generate more flexible magnetic stimuli. Due to the modularity of the CHB inverter, it can be stacked for high-power neuromodulation applications. To generate a flexible magnetic pulse, CHB inverters can synthesize a staircase waveform using the PWM method.

TABLE 3 KEY COMPONENTS OF THE XTMS CIRCUIT

Component	*Nominal Rating*	*Part #*	*Manufacturer*
Step-up transformer	Output: 570 VAC, 10 A Class-E insulation	Custom manufactured	Eastern Transformers, UK
Full bridge diode rectifier	1200 V, Ultrafast recovery diode I_{FRM} [a] = 600 A	STTH9012TV1	STMicroelectronics
Energy storage capacitors	10000 µF, 500 V_{DC} Aluminum Capacitor	ALS70A103NT500	KEMET Electronics
IGBT power module	1.2 kV, I_{CRM} [b] = 1.8 kA	SEMiX603GB12E4p	Semikron, Germany
IGBT gate driver core	$V_{GE\ (on)}$= 15 V, $V_{GE\ (off)}$= -8 V Gate peak current= ±6 A	2SC0106T2A1-12	Power Integrations
Stimulation coil	15.5 µH	D70 Remote Coil	Magstim, UK
Digital controller	PWM generation resolution: 10 ns	Micro Lab Box, includes Power PC Dual Core 2 GHz processor, DS1202, DS1302 I/O	dSPACE, Germany

a. Repetitive peak forward current, tp = 5 µs, F= 5 kHz square

b. Peak current value at collector output during pulse operation

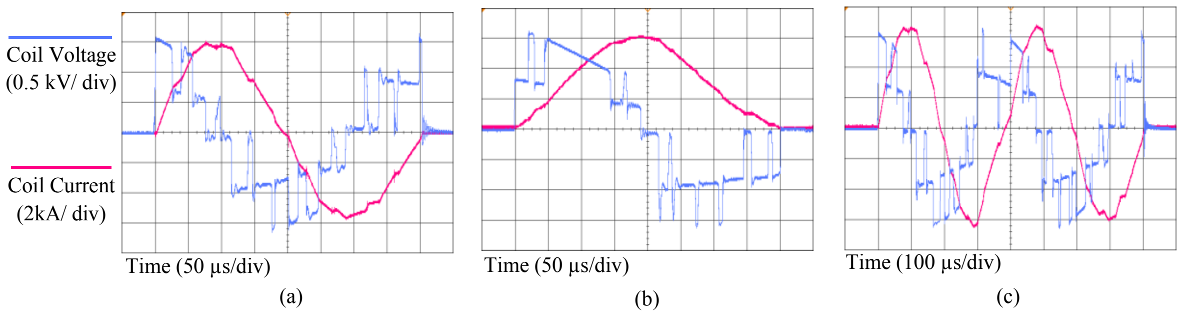

Figure 4 Measured waveforms for three different stimulus shapes. Coil voltage and current for (a) a 2.5 kHz biphasic pulse. (b) a 2.5 kHz monophasic pulse. (c) Two continuous 2.5 kHz biphasic pulses, as an example of the polyphasic pulse.

Similar to the total harmonic distortion (THD) concept in modulation-based power converters, in the proposed xTMS system, a lower L^2 norm means that the inverter block generates a more accurate reproduction of a reference pulse. Increasing the number of CHB leads to the stimulus being closer to the reference signal and reduces the L^2 norm. However, because of the hardware cost and the system complexity, the H-bridge count can only be increased up to a certain number. On the other hand, the results obtained by the mathematical study of the RC neuron model, reveal that the distortion of a PWM stimulus waveform has a limited effect on the neural behavior and can induce an almost identical membrane potential on the neuron, compared to conventional pulses.

Recent experimental research has shown that the activation dynamics of a neuronal population are influenced by the stimulus waveform, pulse width and direction [14] [15]. The induced neuroplastic aftereffects are significantly affected by stimulus parameters such as the pulse shape [16] [17]. A methodical exploration of the effects of different pulse shapes requires the magnetic stimulator to be able to generate the desired pulses with higher flexibility and to combine arbitrary stimuli in repetitive paradigms.

Adding a second H-bridge to the previous generation of this technology (pTMS) increased the maximum output energy of the device from 100.4 J to 250 J and reduced the voltage stress on the IGBTs. One restriction in the cTMS equipment is the high current stress on the power switches as reported in [3]. Although current overload does not necessarily cause the instant failure of the IGBTs, they have been observed to substantially reduce the lifetime of the power switches and to raise the risk of failure [18]. As proposed, paralleling the IGBTs reduces the current stress of the switches and contributes to the reliability and safety of the magnetic pulse generator.

Peterchev et al. utilized two IGBT modules with voltage classes of 1.5 kV and 3.3 kV in the cTMS3 device [3]. Although this selection reduces the required number of IGBT modules and the complexity of the final system, comparing the cost of high voltage class switches with lower voltage ones that are cascaded together, has shown that the cascades topologies are more cost-effective for TMS systems. In addition, cascaded structures, such as the proposed CHB design, give more freedom in generating arbitrary magnetic pulses.

V. Conclusion

This study presents the unique potential of the cascaded H-bridge inverter topologies to generate an arbitrary magnetic stimulus. In particular, the implemented xTMS equipment can produce more flexible and programmable magnetic pulses and protocols, compared to the state-of art TMS equipment. The modular property of the proposed system allows further improvement of the magnetic waveform by cascading H-bridges. The PWM switching patterns enable maximum recovery of the energy transferred to the treatment coil, which permits the generation of rapid rTMS protocols. Non-invasive neurostimulation technologies are moving towards more programmable approaches. Future developments of this versatile xTMS device to apply new modulation paradigms may support novel treatments of neurological and psychiatric disorders.

Acknowledgment

The authors would like to thank Magstim Company Ltd (UK) for providing the stimulation coil, Magstim Rapid² systems, valuable guidance on design considerations, and an MRC iCASE fellowship for Karen Wendt.

References

[1] Y. Zhang and et al., "Identification of psychiatric disorder subtypes from functional connectivity patterns in resting-state electroencephalography," *Nature Biomedical Engineering,* 2020.

[2] M. Memarian Sorkhabi and et al., "Deep-Brain Transcranial Stimulation: A Novel Approach for High 3-D Resolution," *IEEE Access,* vol. 5, pp. 3157 - 3171, 2017.

[3] A. V. Peterchev, K. D'Ostilio, J. C. Rothwell and D. L. Murphy, "Controllable pulse parameter transcranial magnetic stimulator with enhanced circuit topology and pulse shaping.," *Journal of neural engineering,* vol. 22, no. 5, 2014.

[4] M. MemarianSorkhabi and e. al., "Programmable Transcranial Magnetic Stimulation- A Modulation Approach for the Generation of Controllable Magnetic Stimuli," *IEEE Transactions on Biomedical Engineering,* 2020.

[5] W. Gerstner, W. M. Kistler, R. Naud and L. Paninski, Neuronal Dynamics: From single neurons to networks and models of cognition, Cambridge University Press, 2014.

[6] C. E. Corthout, A. Barker and A. Cowey, "Transcranial magnetic stimulation, Which part of the current waveform causes the stimulation?," *Exp Brain Res,* vol. 141, p. 128–132, September 2001.

[7] P. MARIAN, "CHAPTER 5 - Control of PWM Inverter-Fed Induction Motors," in *Control in Power Electronics, Selected Problems*, Academic Press, 2002, pp. 161-207.

[8] A. Barker, C. Garnham and I. Freeston, "Magnetic nerve stimulation: the effect of waveform on efficiency, determination of neural membrane time constants and the measurement of stimulator output.," *Electroencephalogr Clin Neurophysiol Suppl,* vol. 43, pp. 227-37, 1991.

[9] A. V. Peterchev and et al., "Pulse width dependence of motor threshold and input–output curve characterized with controllable pulse parameter transcranial magnetic stimulation," *Clinical Neurophysiology,* vol. 124, no. 7, pp. 1364-1372, 2013.

[10] M. M. Sorkhabi and et al., "Measurement of transcranial magnetic stimulation resolution in 3-D spaces," *Measurement,* vol. 116, pp. 326-340, 2018.

[11] "https://www.mouser.co.uk/ProductDetail/Infineon-Technologies/TD162N16KOF?qs=Pjqho33g6LITOAzemoiDsg%3D%3D," Infineon Technologies. [Online].

[12] "RS," Semikron, [Online]. Available: https://uk.rs-online.com/web/p/igbts/1220393/.

[13] M. Memarian sorkhabi and e. al., "Paralleling Insulated-gate bipolar transistors in the H-bridge structure to reduce current stress," *SN applied science,* no. 3, 2021.

[14] A. Pisoni, A. Vergallito, G. Mattavelli, E. Varoli, M. Fecchio, M. Rosanova, A. G. Casali and L. J. Romero Lauro, "TMS orientation and pulse waveform manipulation activates different neural populations: direct evidence from TMS-EEG," 26 April 2018. [Online]. Available: https://doi.org/10.1101/308981. [Accessed 3 April 2020].

[15] C. EP and et al., "Effects of pulse width, waveform and current direction in the cortex: A combined cTMS-EEG study.," *Brain Stimul.,* vol. 11, no. 5, pp. 1063-1070, 2018.

[16] M. Memarian Sorkhabi and et al., "Numerical Modeling of Plasticity Induced by Quadri-Pulse Stimulation," *IEEE Access ,* vol. 9, pp. 26484 - 26490, 2021.

[17] Y. Shirota and et al., "Strength-Duration Relationship in Paired-pulse Transcranial Magnetic Stimulation (TMS) and Its Implications for Repetitive TMS," *Brain Stimulation,* vol. 9, no. 5, pp. 755-761, 2016.

[18] C. Mauro, "Selected failure mechanisms of modern power modules," *Microelectronics Reliability,* vol. 42, no. 4-5, pp. 653-667, May 2002.